Nonequilibrium phonon effects on the transient high-field transport regime in InP

J. C. Vaissiere, J. P. Nougier, L. Varani, and P. Houlet
Centre d'Electronique de Montpellier, Université Montpellier II, 34095 Montpellier Cedex 5, France

L. Hlou
Faculté des Sciences de Kénitra, Kénitra, Morocco

L. Reggiani
Dipartimento di Scienza dei Materiali ed Istituto Nazionale di Fisica della Materia, Università di Lecce, Via per Monteroni, 73100 Lecce, Italy

P. Kocevar
Institut für Theoretische Physik, Universität Graz, Universitätsplatz 5, A-8010 Graz, Austria
(Received 19 October 1995)

We present a detailed investigation of the transient transport regime in InP at room temperature based on an original method to solve numerically the coupled hot-phonon–hot-carrier time-dependent Boltzmann equations for the case of a steplike high dc electric field pulse. The method enables a study of the perturbation of the phonon distribution function induced by hot carriers and the corresponding modifications of the carrier distribution function. The numerical accuracy of the method is far beyond other existing methods, and, as a consequence, the time behavior of the main transport parameters can be resolved in great detail. The presence of nonequilibrium phonons is found to be responsible for an overall increase in the time duration of the transient regime. Modifications in the time evolution of the main transport parameters are also observed; in particular, the carrier drift velocity exhibits a second overshoot for electric fields near the threshold value for negative differential mobility. The sensitivity of the results to the value of the phonon relaxation time is also discussed.

I. INTRODUCTION

The study of nonequilibrium phonon distributions and their related effect on kinetic coefficients has become a quite established subject in modern solid-state theory.[1–20] As a matter of fact, the energy transferred from an external perturbation, such as an intense light pulse (laser excitation) or a high electric field (nonohmic transport), to a semiconductor is known to drive the carrier system far from its equilibrium (hot-carrier phenomena).[21] If this energy is mainly dissipated through phonon emission, then the phonon population can deviate from its thermal equilibrium value (hot-phonon phenomena). In particular, the phonon distribution function (PDF) can be significantly perturbed when the carrier scattering rate with that particular type of phonons is comparable to the thermalization rates of these phonons.[7] Among cubic semiconductors, III-V compounds are the most suitable materials to evidence the presence of hot phonons through the amplification of longitudinal-optical (LO) phonons, since in these semiconductors the polar-optic carrier-LO phonon couplings are strong and the time constants related to the establishment of phonon thermal equilibrium are sufficiently long.

The influence of hot phonons on carrier transport parameters in polar semiconductors has been theoretically studied in relation with nonohmic transport in bulk material and quantum wells,[19,20] laser photoexcitation,[18,22] and noise phenomena.[23–25] In what concerns the transient transport regime, the influence associated with the presence of highly nonequilibrium optical phonons has been investigated for the first time in Ref. 19 by means of a Monte Carlo simulation of the response of the coupled carrier-phonon system to a steplike onset of a high dc electric field. Nevertheless, a systematic investigation of the effect of a nonequilibrium phonon population on the carrier distribution function (CDF) and the main transport parameters is still lacking in the literature.

In this paper we present a detailed investigation of the transient transport regime in InP at room temperature.

The paper is organized as follows. Section II deals with the theoretical model, first presenting the system of coupled hot-phonon–hot-carrier Boltzmann equations (BE) and thereafter discussing the main problems related to the optimization of the numerical code used to solve it. In Sec. III we provide a validation of the present method by comparing its results for the asymptotic time regime with those obtained by direct solution of the coupled BE under steady-state conditions. In Sec. IV we present the results concerning the CDF, the PDF, and finally those related to the main transport parameters, that is, the mean drift-velocity and energy and the valley populations. Some conclusions are drawn in Sec. V.

II. THEORY

In this section we present the system of coupled hot-phonon–hot-carrier BE which will be solved by means of a numerical simulation. Then, some problems related to the optimization of the numerical code are discussed.

A. The system of coupled Boltzmann equations

To take into account the perturbation of the LO phonon population, it is convenient to write the time-dependent BE for the CDF $f(\mathbf{k},t)$ in the following form:

$$\frac{\partial f(\mathbf{k},t)}{\partial t}=\hat{C}_{\mathrm{rem}}f(\mathbf{k},t)+\hat{C}_{\mathrm{po}}f(\mathbf{k},t). \tag{1}$$

Here, $\hat{C}_{\mathrm{po}}$ is the collision operator associated with polar-optic LO-phonon scattering and $\hat{C}_{\mathrm{rem}}$ is the operator including the external field term and the remaining scattering mechanisms, i.e., acoustic deformation potential, piezoelectric, impurity, and all symmetry-allowed intervalley and intravalley nonpolar optical phonon scatterings. Neglecting degeneracy, the second term in the right-hand side (r.h.s.) of Eq. (1) can be written as

$$\hat{C}_{\mathrm{po}}f(\mathbf{k},t)=\hat{C}'_{\mathrm{po}}f(\mathbf{k},t)-\frac{f(\mathbf{k},t)}{\tau_{\mathrm{po}}(\mathbf{k})}, \tag{2}$$

where $\hat{C}'_{\mathrm{po}}$ is the input term for LO-phonon scattering and $[f(\mathbf{k},t)/\tau_{\mathrm{po}}(\mathbf{k})]$ the output term, $1/\tau_{\mathrm{po}}(\mathbf{k})$ being the rate for carrier-LO-phonon scattering. The detailed expressions for the above operators and rate can be found in Ref. 20.

We remark that (i) $\hat{C}_{\mathrm{po}}$ depends on the PDF and, as a consequence, Eq. (1) becomes nonlinear and time dependent since the deviation of the PDF from its thermal-equilibrium value depends on the instantaneous field-dependent nonequilibrium carrier distribution; (ii) since carrier-carrier interactions and generation-recombination processes with their inherent higher-order density dependencies are neglected, $\hat{C}_{\mathrm{rem}}$ is a linear operator and therefore its associated matrix is independent of time.

The time-dependent phonon BE gives the evolution of the PDF $N(\mathbf{q},t)$ according to

$$\frac{\partial N(\mathbf{q},t)}{\partial t}=\left[\frac{\partial N(\mathbf{q},t)}{\partial t}\right]_{\mathrm{carr}}+\left[\frac{\partial N(\mathbf{q},t)}{\partial t}\right]_{\mathrm{latt}}, \tag{3}$$

where the former term in the r.h.s. of Eq. (3) represents the rate of change due to phonon-carrier interaction and the latter term represents the rate of change due to phonon relaxation toward thermodynamic equilibrium with the lattice temperature T_L. These two terms can be written more explicitly as

$$\left[\frac{\partial N(\mathbf{q},t)}{\partial t}\right]_{\mathrm{carr}}=\hat{C}_{\mathrm{ph}}N(\mathbf{q},t)-\hat{D}_{\mathrm{ph}}N(\mathbf{q},t), \tag{4}$$

$$\left[\frac{\partial N(\mathbf{q},t)}{\partial t}\right]_{\mathrm{latt}}=-\frac{[N(\mathbf{q},t)-N_L]}{\tau_L}, \tag{5}$$

where $\hat{C}_{\mathrm{ph}}$ and $\hat{D}_{\mathrm{ph}}$ are the gain and loss operators related to emission and absorption of phonons by carriers, respectively, N_L is the thermal-equilibrium Planck distribution, and τ_L the phonon relaxation time. The latter can be obtained through a spectroscopically fitted two-channel-decay formula[26] for GaAs, assuming a similar LO-phonon decay dynamics for InP:

$$\tau_L=\frac{\tau_0}{1+\left[\exp\left(\frac{0.65\hbar\omega_{\mathrm{op}}}{K_BT_L}\right)-1\right]^{-1}+\left[\exp\left(\frac{0.35\hbar\omega_{\mathrm{op}}}{K_BT_L}\right)-1\right]^{-1}}. \tag{6}$$

Its zero-temperature limit τ_0, for GaAs, has been found to be in the range 8–20 ps (Refs. 5 and 27–30); $\hbar\omega_{\mathrm{op}}$ denotes the LO-phonon energy and K_B the Boltzmann's constant.

The main task is now to solve the system of coupled equations (1) and (3). To do that, we have devised the following iterative procedure.

(i) The CDF and PDF at thermal equilibrium are introduced in Eqs. (1) and (3), thus calculating $[\partial f(\mathbf{k},t)/\partial t]_{t=0}$ and $[\partial N(\mathbf{q},t)/\partial t]_{t=0}$, just at the onset of the external field at $t=0$.

(ii) From the knowledge of the above quantities we determine $f(\mathbf{k},\Delta t)$ and $N(\mathbf{q},\Delta t)$ by a predictor-corrector method.[31]

(iii) The new CDF and PDF at time Δt are introduced in Eqs. (1) and (3), thus calculating $[\partial f(\mathbf{k},t)/\partial t]_{t=\Delta t}$ and $[\partial N(\mathbf{q},t)/\partial t]_{t=\Delta t}$.

(iv) From the knowledge of these quantities we determine $f(\mathbf{k},2\Delta t)$ and $N(\mathbf{q},2\Delta t)$.

(v) Steps (iii) and (iv) are iteratively repeated until the stationary regime is reached.

B. Numerical simulation

The self-consistent solution of the system of coupled Eqs. (1) and (3) presents several numerical problems. In the present case, the operator associated with the carrier-LO-phonon interaction depends on the PDF, which, as already stated in Sec. IIA, is a time-dependent quantity; therefore, $\hat{C}_{\mathrm{po}}$ must be recalculated at each time step. Furthermore, the inclusion of the BE for the time evolution of the PDF is found to significantly increase the duration of the transient regime. We shall come back to this aspect in the following. This makes it imperative to optimize the numerical algorithms in order to save computer time. Let us briefly describe this optimization procedure.

Concerning the carrier BE, we notice that Eq. (1) can be written in matrix form as

$$\left[\frac{\partial f}{\partial t}\right]=[C]_{\mathrm{rem}}[f]+[C']_{\mathrm{po}}[f]+\left[\frac{1}{\tau_{\mathrm{po}}}\right][f], \tag{7}$$

where $[C']_{\mathrm{po}}$ and $[1/\tau_{\mathrm{po}}]$ are the matrices associated with the LO-phonon scattering operator depending on time through the PDF, and $[C]_{\mathrm{rem}}$ is the time-independent matrix associated with the operator $\hat{C}_{\mathrm{rem}}$. The calculation of the first two matrices is the part of the program which requires most of the computer time. Indeed, since the time duration of the transient regime is of about 20 ps and the time step of the simulation is typically $\Delta t=1\,fs$, this calculation must be performed about 2×10^4 times. To try to avoid such a numerical expenditure, we have verified that the increase in the time duration of the transient is due to the slow time variation of the PDF with respect to that of the CDF. Therefore, the time-dependent matrices have been recalculated *only* when the PDF has undergone a significant variation (about 1%). As a

consequence, the calculation of the time-dependent matrices is typically performed each 20 Δt, thus significantly reducing the computation time.

Concerning the phonon BE, we remark that Eq. (3) can be more explicitly written as

$$\frac{\partial N(\mathbf{q},t)}{\partial t}=\left[\frac{2\Omega}{8\pi^3}\int_{\mathbf{k}} f(\mathbf{k},t)C(\mathbf{q},\mathbf{k})d\mathbf{k}\right][N(\mathbf{q},t)+1] -\left[\frac{2\Omega}{8\pi^3}\int_{\mathbf{k}} f(\mathbf{k},t)D(\mathbf{q},\mathbf{k})d\mathbf{k}\right]N(\mathbf{q},t)-\frac{N(\mathbf{q},t)}{\tau_L} +\frac{N_L}{\tau_L}, \tag{8}$$

where Ω is the crystal volume, the first term on the r.h.s. corresponds to $\hat{C}_{\rm ph}N(\mathbf{q},t)$, and the second term to $\hat{D}_{\rm ph}N(\mathbf{q},t)$, $C(\mathbf{q},\mathbf{k})$ and $D(\mathbf{q},\mathbf{k})$ being appropriate functions whose explicit expressions can be found in Ref. 20. By adjusting the different terms in Eq. (8), we obtain

$$\frac{\partial N(\mathbf{q},t)}{\partial t}=\left[\frac{2\Omega}{8\pi^3}\int_{\mathbf{k}} f(\mathbf{k},t)A(\mathbf{q},\mathbf{k})d\mathbf{k}\right]N(\mathbf{q},t) +\frac{2\Omega}{8\pi^3}\int_{\mathbf{k}} f(\mathbf{k},t)C(\mathbf{q},\mathbf{k})d\mathbf{k}-\frac{N(\mathbf{q},t)}{\tau_L}+\frac{N_L}{\tau_L}, \tag{9}$$

where $A(\mathbf{q},\mathbf{k})=C(\mathbf{q},\mathbf{k})-D(\mathbf{q},\mathbf{k})$. The two integrals on the r.h.s. of Eq. (9) can be performed by discretizing the values of $\mathbf{q}$ and $\mathbf{k}$ in $(\mathbf{q},\mathbf{k})$-space, thus obtaining

$$\frac{\partial N(q_i,t)}{\partial t}=\left[\frac{2\Omega}{8\pi^3}\sum_j \alpha_j f(k_j,t)A(q_i,k_j)\right]N(q_i,t) +\frac{2\Omega}{8\pi^3}\sum_j \gamma_j f(k_j,t)C(q_i,k_j)-\frac{N(q_i,t)}{\tau_L}+\frac{N_L}{\tau_L}, \tag{10}$$

where α_j and γ_j are appropriate coefficients. With a more compact notation we can write

$$\frac{\partial N_i(t)}{\partial t}=\left[\sum_j E_{ij}f_j(t)\right]N_i(t)+\sum_j F_{ij}f_j(t)-\frac{N_i(t)}{\tau_L}+\frac{N_L}{\tau_L}. \tag{11}$$

The coefficients E_{ij} and F_{ij} are independent of the CDF and therefore independent of time: This enables us to calculate the matrices $[E]$ and $[F]$ only once at the beginning of the simulation, thus saving another significant amount of computer time.

By using the optimization procedures described above, the CPU time of a typical simulation is reduced from 120 h to about 6 h.

C. Physical model

The theory is applied to the case of n-type InP at temperature $T_L=300$ K, with a doping concentration $N_D=10^{17}$ cm^{-3}, using the same material parameters as reported in Appendix B of Ref. 20. Two types of spherical and nonparabolic valleys (Γ and L) are taken into account[32] so that we take advantage of the use of cylindrical symmetry. The simulation includes the following intra- and intervalley scattering mechanisms: acoustic deformation potential (in elastic approximation),[33–35] acoustic piezoelectric (in elastic approximation),[36–38] polar optical,[36,39,40] ionized-impurity (in the Brooks-Herring approximation including a screened Coulomb potential)[41–43] and nonpolar intervalley scattering.[44,45] The zero-temperature LO-phonon relaxation time τ_0, extrapolated from measurements on GaAs, has been taken equal to 16 ps.[46] From this choice of τ_0 and for $T_L=300$ K and $\hbar\omega_{\rm LO}=43.2$ meV, we obtain $\tau_L=5.8$ ps.

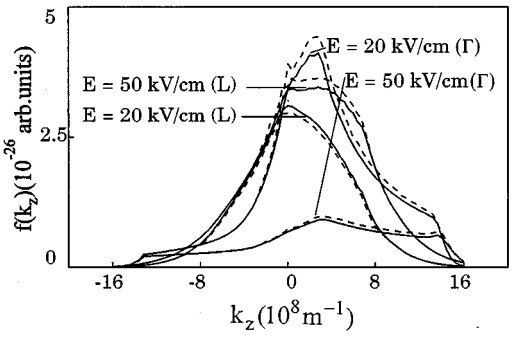

FIG. 1. Carrier distribution functions $f(k_z)=f(k_x=0,\ k_y=0,\ k_z)$ in the Γ and L valleys as functions of k_z along the electric field in InP for $T_L=300$ K, $N_D=10^{17}$ cm^{-3}, and the reported electric fields. The continuous lines refer to calculations performed with the stationary iterative method (Ref. 20) and the dashed lines to calculations performed with the presently developed transient iterative method at 20 ps from the beginning of the dc field pulse.

III. VALIDATION OF THE METHOD

To check the validity of the numerical procedure illustrated in the previous section, we have performed a comparison between the results obtained with the present method for a time longer than the duration of the transient and the results obtained by directly solving the system of coupled hot-phonon–hot-carrier BE under stationary conditions.[20,47]

Figure 1 reports the CDF in the Γ and L valleys for the two electric fields of 20 and 50 kV/cm, both above the threshold value for negative differential mobility of about 10 kV/cm. Due to the presence of the high electric field, in both valleys the CDF exhibits various structures related to the different microscopic scattering mechanisms: As a matter of fact, the kinks of the CDF in the Γ valley at high $|k_z|$ are associated with the intervalley phonons, while its maximum is associated with the LO-phonon scattering as the dominant momentum- and energy-dissipation mechanism.

Figure 2 reports the PDF at three different electric fields obtained with the two methods. Following the expectations, we observe that the perturbation of the PDF increases with increasing electric field strength. In agreement with previous studies,[18–20,22] the region at the smallest phonon wave vectors q is not modified, while the distortion of the CDF at high k values related to intervalley transfer has been found to be responsible for the appearance of two narrow peaks in the PDF at low q values, (the peak in the positive q region being higher than the peak in the negative q region due to the

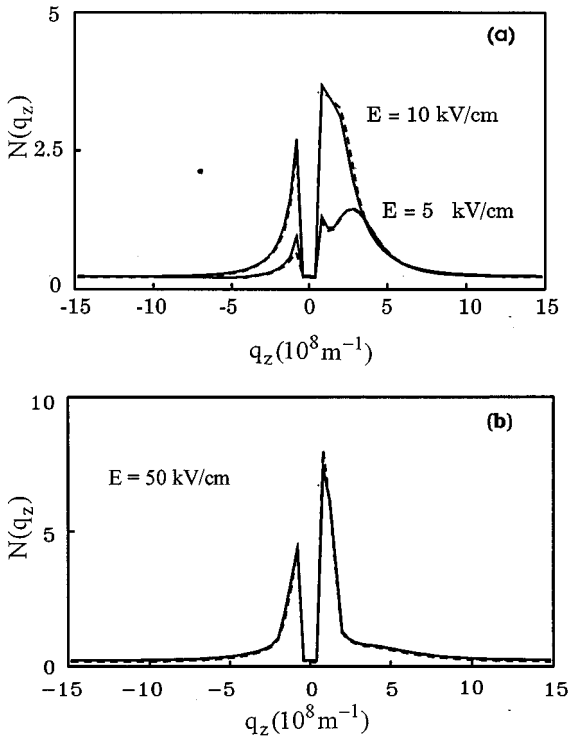

FIG. 2. Phonon distribution function $N(q_z)=N(q,\theta=0)$ as a function of q_z along the electric field in InP for $T_L=300$ K, $N_D=10^{17}$ cm^{-3}. The continuous lines refer to calculations performed with the stationary iterative method (Ref. 20) and the dashed lines to calculations performed with the presently developed transient iterative method at 20 ps from the beginning of the dc field pulse. (a) $E=5$ and 10 kV/cm; (b) $E=50$ kV/cm.

higher values of the CDF in the positive k region).[20] The third and wider peak observed in Fig. 2(a) at larger positive q values is associated wit the overall heating of the CDF; by increasing the electric field strength, this peak shifts to smaller q values until merging with the nearest one, as shown in Fig. 2(b). We note the excellent agreement between the CDF and the PDF obtained with the two different methods which validates the present numerical procedure.

From the knowledge of the CDF we have evaluated the two transport parameters, carrier drift-velocity and energy, which are reported in Fig. 3. It is evident that the general agreement found for the CDF in the whole range of electric fields reflects itself on a general agreement concerning the different transport parameters which are obtained as integrals of the CDF. The same good agreement has been found also on the Γ- and L-valley populations.

IV. RESULTS UNDER TRANSIENT REGIME

Taking advantage of the above agreement, we can now investigate in detail the results under transient regime. We first present the results concerning the CDF and the PDF. Thereafter, we discuss the results related to the main transport parameters, i.e., drift-velocity, energy, and valley populations. To better evidence the effect of the nonequilibrium phonons, in all cases the results assuming phonons at thermal equilibrium are shown as well. Finally, the effect of the choice of the phonon relaxation time is discussed.

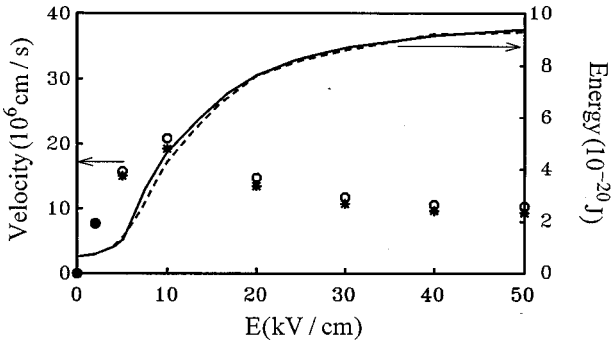

FIG. 3. Average drift velocity and average carrier energy as functions of the electric field in InP for $T_L=300$ K, $N_D=10^{17}$ cm^{-3}, computed with nonequilibrium phonons. The stars and the continuous line refer to calculations performed with the stationary iterative method (Ref. 20) and the open circles and the dashed line to calculations performed with the presently developed transient iterative method at 20 ps from the beginning of the dc field pulse.

A. Carrier distribution function

When studying the transient regime, carriers are initially taken at thermal equilibrium. Then, under the application of an external electric field, they begin to evolve by populating higher energy regions. Figures 4 and 5 report the CDF in the Γ and L valley, respectively, at different times from the beginning of the transient and for an applied electric field of 10 kV/cm, which is the threshold field for negative differential mobility in InP. Previous studies have evidenced that in this region the effect of hot phonons is more pronounced.[20] Phonon amplification is strictly related to a relative increase of phonon emissions over absorption. For this to occur, the CDF has also to be different from the distribution function at thermal equilibrium. As the phonon disturbance scales with the hot-carrier density, even a relatively weak field is sufficient to perturb the PDF provided the doping concentrations are high enough. Since some time is required to shift the PDF from its equilibrium value, we notice that for times shorter than 0.4 ps no difference is observed between the values of the CDF (continuous lines) and those obtained assuming phonons to be at thermal equilibrium (dashed lines). For times longer than 0.4 ps the two CDF begin to differ, the difference becoming more evident at increasing times. Since for the electric field of 10 kV/cm the presence of nonequilibrium phonons increases the Γ to L transfer,[20] the Γ valley CDF in the presence of hot phonons takes values lower than those without hot phonons [Fig 4(b)], while the opposite behavior is exhibited by the CDF in the L valley [Fig. 5(b)]. We notice also that the presence of a nonequilibrium phonon population is responsible for an increase in the time duration of the transient: This is clearly shown in Figs. 4(b) and 5(b). As a matter of fact, while the CDF calculated without hot phonons reaches the stationary regime in about 4 ps, the CDF calculated with hot phonons is still evolving after a time of 8 ps [see Figs. 4(b) and 5(b)]. We have verified that the duration of the transient in the presence of nonequilibrium phonons reaches about 20 ps. Furthermore, we notice that the presence of hot phonons is found to be responsible for the suppression of the forward peak in the CDF of the Γ valley [see Fig. 4(b)]. The reason is that the initial CDF is peaked at energies below the LO-phonon-emission threshold,

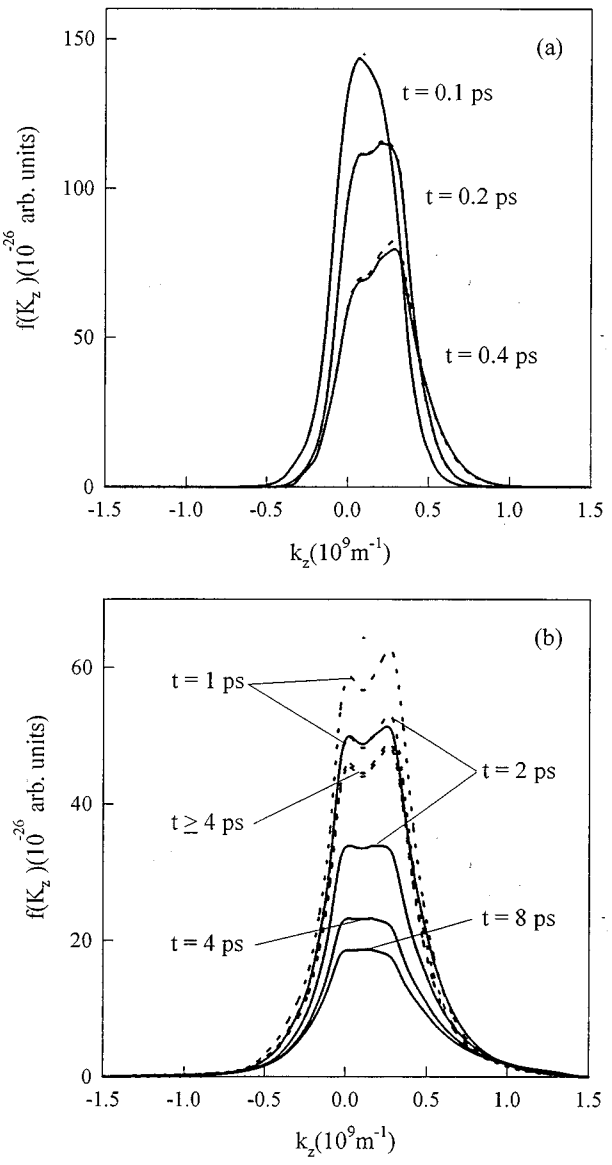

FIG. 4. Carrier distribution function $f(k_z)=f(k_x=0,\ k_y=0,\ k_z)$ as a function of k_z along the electric field, in the Γ valley of InP, for $T_L=300$ K, $N_D=10^{17}$ cm^{-3}, and the reported times after the beginning of the dc field pulse. The solid lines refer to calculations taking into account nonequilibrium phonons and the dashed lines to calculations performed assuming phonons to be a thermal equilibrium. (a) Carrier distribution function at $t=0.1$, 0.2, and 0.4 ps; (b) carrier distribution function at $t=1$, 2, 4, and 8 ps.

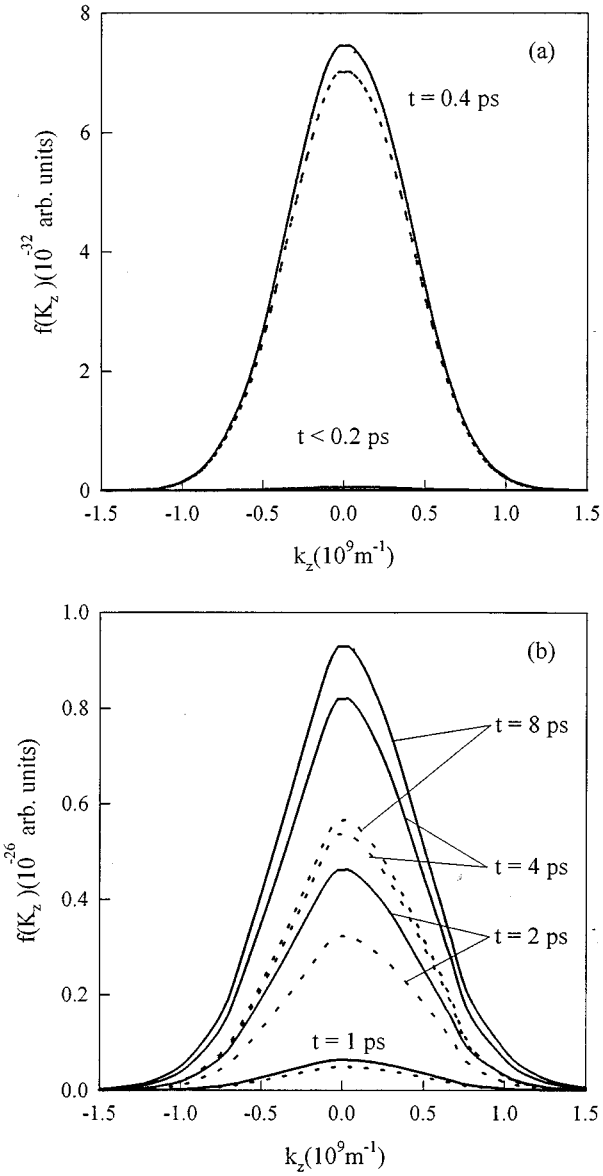

FIG. 5. Carrier distribution function $f(k_z)=f(k_x=0,\ k_y=0,k_z)$ as a function of k_z along the electric field, in the L valley of InP, for $T_L=300$ K, $N_D=10^{17}$ cm^{-3}, and the reported times from the beginning of the dc field pulse. The solid lines refer to calculations taking into account nonequilibrium phonons and the dashed lines to calculations performed assuming phonons to be at thermal equilibrium. (a) Carrier distribution function at $t<0.2$ and at 0.4 ps; (b) carrier distribution function at $t=1$, 2, 4 and 8 ps.

which, after the phonon buildup, leads to a pronounced depletion of these carrier states by phonon reabsorption.[19] No significant change is observed in the shape of the CDF in the L valleys [see Fig. 5(b)], due to the much broader carrier population of these band minima.

B. Phonon distribution function

Figures 6(a)–6(c) report the results of the PDF at different times from the beginning of the transient and for an electric field of 10 kV/cm. Figures 6(a) and 6(b) show a three-dimensional plot of the PDF $N(q,\theta)$, where q is the modulus of the phonon wave vector and θ is the angle between the phonon wave vector and the electric field. Note that in Figs. 6(a) and 6(b) the different curves contain different vertical scales; in order to demonstrate the direct time evolution of the PDF, Fig. 6(c) shows a cut of the PDF along the direction of the electric field, i.e., $N(q_z)=N(q,\theta=0)$ for different times. The perturbation of the PDF is related to the displacement of carriers in the high-energy region. At the shortest times from the beginning of the transient, the CDF is ballistically displaced under the action of the electric field; as a consequence, the PDF develops a peak at small positive q_z associated with the phonons emitted by carriers at high energy. This peak progressively increases with time due to the enhanced LO-phonon emission by carriers. We notice that

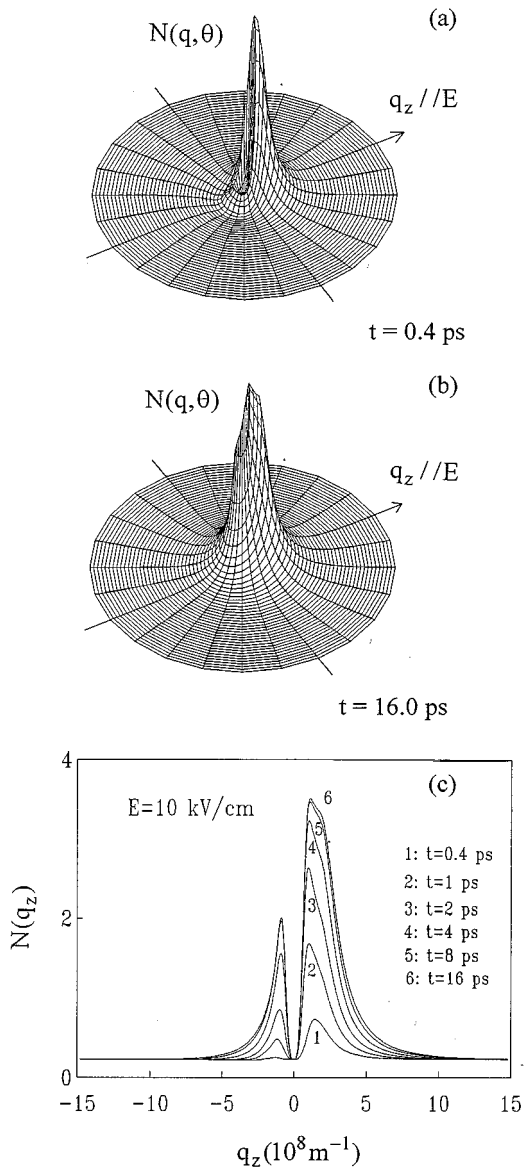

FIG. 6. Phonon distribution function $N(q,\theta)$ in InP, for $T_L=300$ K, $N_D=10^{17}$ cm^{-3}, $E=10$ kV/cm, and the reported times from the beginning of the dc field pulse. (c) refers to the phonon distribution function $N(q_z)=N(q,\theta=0)$ for the phonon wave vector along the electric field.

the shape of the PDF is quite asymmetric at short times [Fig. 6(a)], this asymmetry decreasing at increasing times [Fig. 6(b)]. This can be explained by comparing the PDF with the corresponding CDF reported in Figs. 4 and 5: As a matter of fact, for short times, the CDF is quite asymmetric since the presence of the electric field produces mostly a rigid displacement of the CDF. At longer times, when scatterings begin to take place, the CDF becomes more distributed in k space, thus reducing the asymmetry in the PDF.

C. Transport parameters

To investigate the effect of nonequilibrium phonons on transport parameters in the transient regime, Figs. 7–9 compare mean drift velocities, energies and valley populations as functions of time obtained with phonons at thermal equilibrium (dotted curves) and take phonon disturbances into account (continuous curves).

Figures 7(a)–7(c) report the results for the drift velocity in the Γ valley and L valley and the average drift velocity for three electric fields of 5, 10, and 20 kV/cm. At the shortest times ($\leqslant 0.4$ ps) there is practically no difference between the values of the drift velocity obtained with and without hot phonons; this is related to the fact that some time is required for the perturbation of the PDF to develop after the CDF has deviated from its standard evolution under the condition of phonons at thermal equilibrium (see Figs. 4 and 5). Thereafter, a modification in the time evolution of the drift velocity is observed, which finally leads to the difference of the values in the stationary regime already discussed in Sec. III (see Fig. 3). Since phonons are mainly absorbed by carriers having their velocity in the direction of the electric field,[20] in the case of high electric fields the intervalley transfer is increased by the interplay between an LO-phonon absorption by carriers just below the intervalley-scattering threshold and an immediately following Γ-L scattering; as a consequence, the overall drift velocity tends to decrease. In the case of small electric fields the nonequilibrium-phonon-induced increase of the mean drift velocity v_Γ in the Γ valley is not overcompensated by intervalley transfers, thus producing a continuous increase of the mean drift velocity. An interesting effect is noticed in the transient regime of v_Γ [Fig. 7(a)], where, for an intermediate electric field of 10 kV/cm, a second overshoot is observed which reaches its maximum at times around 2 ps. This second overshoot can be ascribed to the following mechanism: As the net increase of LO-phonon reabsorption is due to carriers at the bottom of the band (below the phonon-emission threshold), this results in an overpopulation of carrier states with forward **k** vector due to the reabsorption of LO phonons with the wave vector parallel to the field direction. A rough estimate of the time it takes the field to carry these states to Γ-L-transfer threshold region gives 3 ps, in agreement with the position of the second overshoot in Fig. 7(a). For times much longer than 2 ps the asymmetry in the perturbed PDF is reduced, as already discussed in Sec. IV B (see Fig. 6). We notice that the transient regime of the drift velocity v_L in the L valley is not significantly modified by the presence of hot phonons apart from the difference in the stationary values. The small overshoot at the shortest times in Fig. 7(b) is related to a small amount of Γ-L transfer during the first time steps when the carrier concentration in these valleys is still the very small equilibrium one (about 10^{-8}%).[47] We observe that the time evolution of the average drift velocity reported in Fig. 7(c) follows nearly that of v_Γ except for the highest electric field of 20 kV/cm, where, due to the enhancement of the L-valley population, the difference between the time evolution of the drift velocity with and without hot phonons is reduced.

Figure 8 reports the results of the carrier energy in the Γ valley [Fig. 8(a)], in the L valley [Fig. 8(b)], and the total [Fig. 8(c)] for the same electric fields of Fig. 7. Also in this case the presence of nonequilibrium phonons is found to be responsible for modifications in the time evolution in the transient regime. As already noticed for the case of the drift velocity, these modifications appear after the time required for the perturbation of the PDF to take place. After the initial

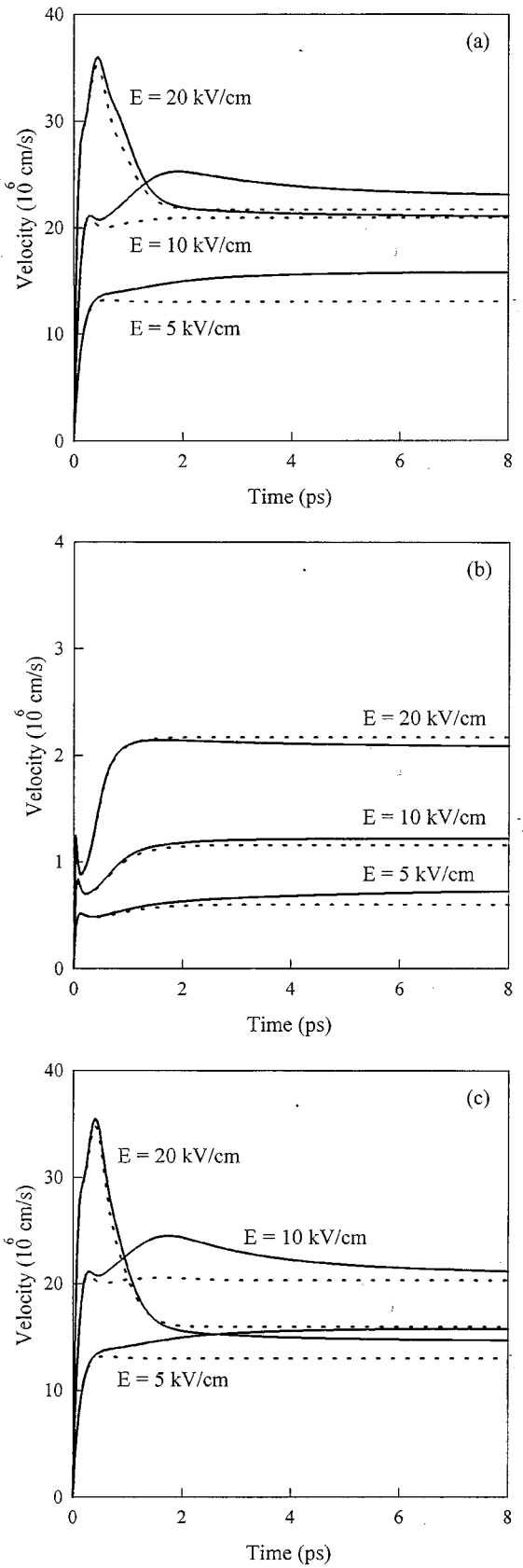

FIG. 7. Mean carrier drift velocity as a function of time in InP, for $T_L = 300$ K, $N_D = 10^{17}$ cm^{-3}, and the reported electric fields. The solid lines refer to calculations taking into account nonequilibrium phonons and the dashed lines to calculations performed assuming phonons to be at thermal equilibrium. (a) Mean drift velocity in the Γ valley; (b) mean drift velocity in the L valley; (c) average mean drift velocity.

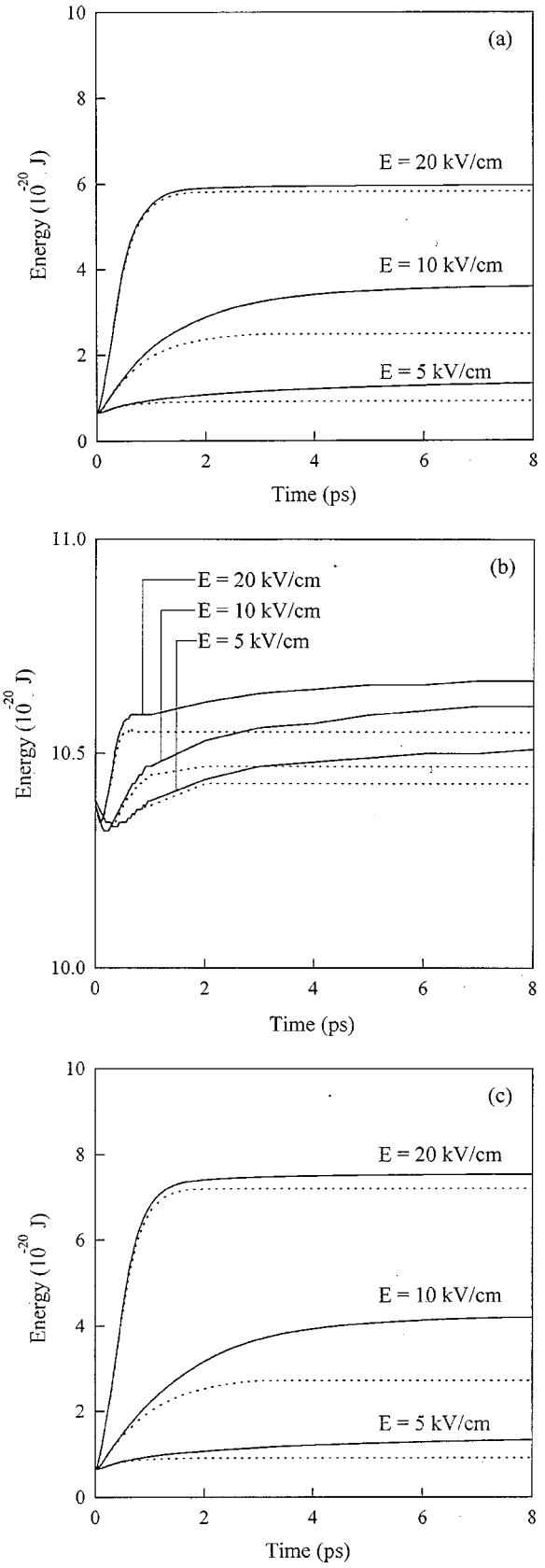

FIG. 8. Mean carrier energy as a function of time in InP, for $T_L = 300$ K, $N_D = 10^{17}$ cm^{-3}, and the reported electric fields. The solid lines refer to calculations taking into account nonequilibrium phonons and the dashed lines to calculations performed assuming phonons to be at thermal equilibrium. (a) Mean energy in the Γ valley; (b) mean energy in the L valley; (c) average energy.

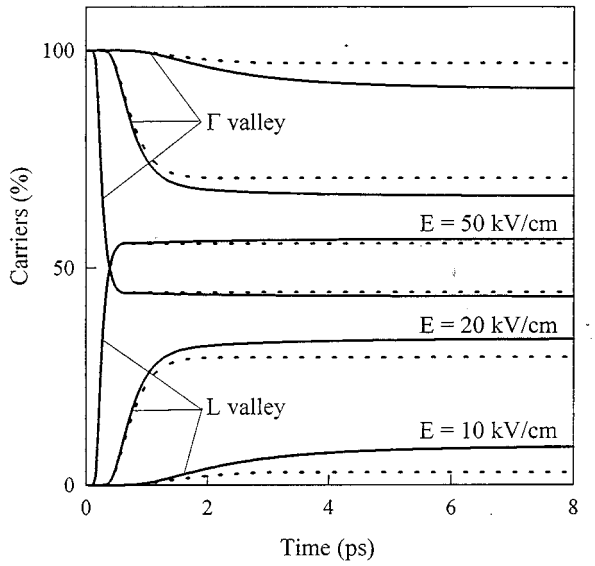

FIG. 9. Occupation of the Γ and L valleys as a function of time in InP for $T_L=300$ K, $N_D=10^{17}$ cm^{-3}, and the reported electric fields. The solid lines refer to calculations taking into account nonequilibrium phonons and the dashed lines to calculations performed assuming phonons to be a thermal equilibrium.

stage, a modification in the time evolution of the energy is observed, which finally leads to the difference of the values in the stationary regime already discussed in Sec. III (see Fig. 3). In the L valley the carrier energy starts initially to decrease due to the small amount of transfers from the Γ valley at the very earliest times which is also responsible for the overshoot of the drift velocity in the L valley previously discussed.[47]

Figure 9 reports the valley populations at the three electric fields of 10, 20, and 50 kV/cm. the presence of nonequilibrium phonons leads finally to different valley populations in the stationary regime, this effect being more pronounced near the threshold field, because in this range of electric field the presence of hot phonons most effectively increases the Γ to L transfer.

To complement our analysis, we have performed a systematic study on the influence of the magnitude of the phonon relaxation time τ_L. Its value is known with an uncertainty related to the value obtained experimentally for τ_0, which for GaAs is in the range 8–20 ps. Therefore, to estimate the effect of the choice of τ_L on transport parameters, we have calculated the transient drift velocity and energy for the two extreme cases (8 and 20 ps) and for an electric field of 5 kV/cm, which gives the greatest nonequilibrium-phonon effects. The results are presented in Figs. 10 and 11. By increasing the value of τ_0, the characteristic phonon thermalization rate decreases, thus enhancing the perturbation of the PDF. As a result, the difference between the values obtained with and without phonon disturbances increases, especially for the mean carrier energies. In any case, no significant modification in the time behavior of both transport parameters is observed.

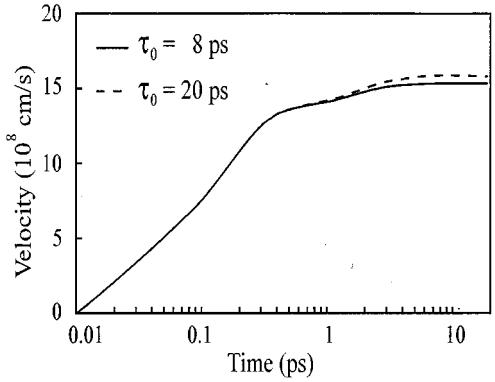

FIG. 10. Mean carrier drift velocity as a function of time in InP, for $T_L=300$ K, $N_D=10^{17}$ cm^{-3}, and $E=5$ kV/cm. The solid line refers to calculations with a zero-temperature phonon-relaxation time $\tau_0=8$ ps and the dashed line to calculations with $\tau_0=20$ ps.

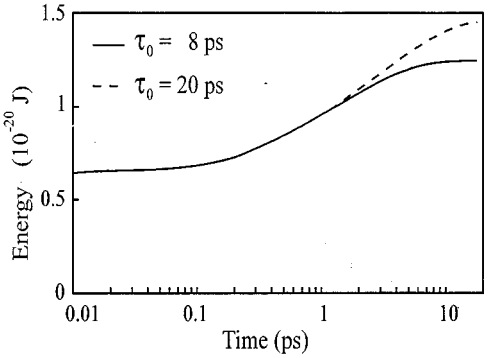

FIG. 11. Mean carrier energy as a function of time in InP for $T_L=300$ K, $N_D=10^{17}$ cm^{-3}, and $E=5$ kV/cm. The solid line refers to calculations with a zero-temperature phonon-relaxation time $\tau_0=8$ ps and the dashed line to calculations with $\tau_0=20$ ps.

V. CONCLUSIONS

We have presented a detailed investigation of the transient high-field transport regime in InP at room temperature after the onset of a dc field pulse. To this end we have proposed a numerical method which solves the coupled hot-phonon–hot-carrier Boltzmann equations in quite an efficient way. The accuracy of the method is particularly evident in the transient transport regime which is fundamental to the performances of high-frequency semiconductor devices. A great effort has been made in order to optimize the code and reach affordable CPU times. To validate our algorithm, we have performed a comparison between the results obtained with the present method for a time longer than the duration of the transient and those obtained by solving directly the system of coupled hot-phonon–hot-carrier Boltzmann equations under stationary conditions. After this validation, we have analyzed the transient transport regime by calculating the carrier distribution function, the phonon distribution function, and the mean drift velocity and carrier energy and the valley populations. The main results are summarized as follows.

(i) The coupling of the carrier Boltzmann equation to the phonon Boltzmann equation is responsible for an increase in the time duration of the transient of the carrier distribution function related to the nonelectronic phonon-relaxation rate.

(ii) At short times after the beginning of the transient, the

phonon distribution function develops a strong forward peak which is related to the displacement of the carrier distribution function caused by the presence of the electric field. At later times, when scatterings begin to play a role, this asymmetry is reduced as a consequence of the spreading of the carrier distribution function.

(iii) In the presence of nonequilibrium phonons the transient regime of the carrier drift velocity is modified, in particular showing a second overshoot at moderately high electric fields.

(iv) In the presence of nonequilibrium phonons also the transient regime of the mean carrier energy is modified, finally leading to an overall increase of the mean carrier energy in the stationary regime.

(v) The time evolution of the valley populations is modified by the enhanced Γ to L transfer induced by hot phonons.

(vi) The magnitude of the modifications of transport parameters in the transient regime has been found to be sensitive to the value of the nonelectronic phonon relaxation time, even if no significant modification of their general behavior has been observed.

ACKNOWLEDGMENTS

This work has been performed within the European Laboratory for Electronic Noise (ELEN) supported by the Commission of European Community through the Contracts Nos. ERBCHRXCT920047 and ERBCHBICT920162. Partial support from the Centre National Universitaire Sud de Calcul (CNUSC), the French Ministère des Affaires Etrangères (MAE) through the Contract GALILÉE, and the Italian Consiglio Nazionale delle Ricerche (CNR) is gratefully acknowledged.

[1] R. Peierls, Ann. Phys. (Leipzig) **4**, 121 (1930); **5**, 244 (1930); **12**, 154 (1932).
[2] P. G. Klemens, Proc. Phys. Soc. London Ser. A **64**, 1030 (1951).
[3] E. H. Sondheimer, Proc. R. Soc. London Ser. A **234**, 391 (1956).
[4] J. E. Parrot, Proc. Phys. Soc. London **70**, 590 (1957).
[5] J. Shah, R. C. C. Leite, and J. F. Scott, Solid State Commun. **8**, 1089 (1970).
[6] P. Kocevar, J. Phys. C **5**, 3349 (1972).
[7] P. Kocevar, in *Physics of Nonlinear Transport in Semiconductors*, Vol. 52 of *NATO Advanced Study Institute*, edited by D. K. Ferry, J. R. Barker, and C. Jacoboni (Plenum, New York, 1980), p. 401.
[8] M. Pugnet, J. Collet, and A. Cornet, Solid State Commun. **38**, 531 (1981).
[9] W. Pötz and P. Kocevar, Phys. Rev. B **28**, 7040 (1983).
[10] K. Kash, J. Shah, D. Block, A. C. Gossard, and W. Wiegmann, Physica B **143**, 189 (1985).
[11] P. Kocevar, Physica B+C **143**, 155 (1985).
[12] P. J. Price, Physica B **143**, 165 (1985).
[13] J. F. Ryan, R. A. Taylor, A. J. Turberfield, and J. M. Worlock, Surf. Sci. **170**, 511 (1986).
[14] V. L. Gurevich, *Transport in Phonon Systems* (North-Holland, Amsterdam, 1986).
[15] P. Bordone, C. Jacoboni, L. Reggiani, and P. Kocevar, J. Appl. Phys. **61**, 1460 (1987).
[16] P. Kocevar, in *Festkörperprobleme* (*Advances in Solid State Physics*), edited by P. Grosse (Pergamon, Braunschweig, 1987), Vol. 27, p. 197.
[17] K. Leo, W. W. Rühle, H. J. Queisser, and K. Ploog, Phys. Rev. B **37**, 7121 (1988).
[18] P. Lugli, P. Bordone, L. Reggiani, M. Rieger, P. Kocevar, and S. M. Goodnick, Phys. Rev. B **39**, 7852 (1989).
[19] M. Rieger, P. Kocevar, P. Lugli, P. Bordone, L. Reggiani, and S. M. Goodnick, Phys. Rev. B **39**, 7866 (1989).
[20] J. C. Vaissiere, J. P. Nougier, P. Fadel, L. Hlou, and P. Kocevar, Phys. Rev. B **46**, 13 082 (1992).
[21] L. Reggiani, *Hot Electron Transport in Semiconductors*, Topics in Applied Physics Vol. 58 (Springer-Verlag, Berlin, 1985).
[22] P. Lugli, Solid-State Electron. **31**, 667 (1988).
[23] R. P. Jindal and A. Van Der Ziel, J. Appl. Phys. **52**, 2884 (1981).
[24] R. Barkauskas, S. V. Gantsevich, V. D. Kagan, and R. Katilius, Sov. Phys. JETP **60**, 187 (1984).
[25] P. Bordone, L. Varani, L. Reggiani, L. Rota, and T. Kuhn, Appl. Phys. Lett. **63**, 1107 (1993).
[26] J. Menendez and M. Cardona, Phys. Rev. B **29**, 2051 (1984).
[27] J. P. Aubert, J. C. Vaissière, and J. P. Nougier, J. Appl. Phys. **56**, 1128 (1984).
[28] R. K. Chang, J. M. Ralston, and D. E. Keating, in *Proceedings of the International Conference on Scattering Spectra in Solids*, edited by C. B. Wright (Springer-Verlag, New York, 1969), p. 369.
[29] D. Von der Linde, J. Kuhl, and H. Klingenberg, Phys. Rev. Lett. **44**, 1505 (1980).
[30] A. Mooradian, in *Laser Handbook*, edited by F. T. Arecchi and E. D. Schutz du Bois (North-Holland, Amsterdam, 1972), p. 1410.
[31] B. A. Lebwohl, P. M. Marcus, Solid State Commun. **9**, 1671 (1971).
[32] E. M. Conwell and M. O. Vassel, Phys. Rev. **166**, 797 (1968).
[33] E. G. S. Paige, Prog. Semicond. **8**, 62 (1964).
[34] J. Bardeen and W. Shockley, Phys. Rev. **80**, 72 (1950).
[35] C. Herring and E. Vogt, Phys. Rev. **101**, 944 (1956).
[36] E. M. Conwell, *High Field Transport in Semiconductors* (Academic, New York, 1967).
[37] B. R. Nag, Solid State Commun. **11**, 987 (1972).
[38] R. S. Crandall, Phys. Rev. B **1**, 730 (1970).
[39] W. A. Harrison, Phys. Rev. **104**, 1281 (1956).
[40] P. Lawaetz, Phys. Rev. **183**, 730 (1971).
[41] H. Brooks and C. Herring, Phys. Rev. **83**, 879 (1951).
[42] H. Brooks, Adv. Electron. Electron. Phys. **7**, 85 (1955).
[43] B. K. Ridley, J. Phys. C **10**, 1589 (1977).
[44] M. Lax and J. J. Hopfield, Phys. Rev. **104**, 128 (1956).
[45] H. W. Streitwolf, Phys. Status Solidi **37**, K47 (1970).
[46] T. C. Damen, R. C. C. Leite, and J. Shah, in *Proceedings of the Tenth International Conference on the Physics of Semiconductors*, edited by S. P. Keller, J. C. Hensel, and F. Spern (U.S. Atomic Energy Commission, Cambridge, MA 1970), p. 735.
[47] J. C. Vaissière, M. Elkssimi, and J. P. Nougier, Semicond. Sci. Technol. **7**, B308 (1992).